Simulation of X-ray Absorption Near Edge Spectra of Organometallic Compounds in the Ground and Optically Excited States

R. K. Pandey and Shaul Mukamel*

Department of Chemistry, University of California, Irvine, California 92697-2025

Received: May 2, 2006; In Final Form: October 20, 2006

The Mg K-edge and Zn K- and L_3-edge X-ray absorption near edge spectra of Mg and Zn porphyrins in the ground state and low-lying optically excited states are calculated. Also computed are X-ray absorption near edge spectra of Fe(II) spin crossover compound in its ground and low-lying optically excited states, motivated by a recent experiment (*J. Phys. Chem. A* **2006**, *110*, 38). The calculated absorption spectra of optically excited states can be used to simulate ultrafast optical pump/X-ray probe experiments.

I. Introduction

Porphyrins form an important class of conjugated chromophores in which a central transition metal atom is surrounded by ligands with nitrogen atoms as nearest neighbors. They play a major role in many biological processes such as photosynthesis (chlorophyll) and oxygen binding (hemoglobin). X-ray absorption of iron hemoproteins,[1,2] zinc sites in proteins,[3] copper and iron porphyrins,[4−6] experimental[7] and theoretical[8] studies of Cu L X-ray absorption spectrum of copper phthalocyanine (CuPc) using the so-called full core hole (FCH) within the density functional theory (DFT) have been reported. The photophysics and photochemistry of nickel porphyrin were studied experimentally by Kim et al.[9,10] Time-resolved study of nickel tetraphenylporphyrin (NiTPP) was carried out experimentally.[11−13] Theoretical study of NiTPP was carried out by Campbell et al.[14] X-ray absorption near edge spectroscopy (XANES) can measure variations in electronic structure due to changes in atomic positions (geometry) and charge distributions of transient species, during and after photoexcitation. This region of the X-ray absorption spectra of up to ∼20 eV above the absorption threshold gives information about the unoccupied density of states of a molecule in the vicinity of the absorbing atom. These states are important for the formation of chemical bonds.

In this paper, we simulate XANES spectra of magnesium porphyrin (MgP) and zinc porphyrin (ZnP) in the ground and low-lying optically excited states. Optical properties of Mg and Zn porphyrins have been measured[15−24] and calculated,[25−31] using the powerful methodologies of DFT. The X-ray spectra have been studied as well.[32,33] Tanida et al. employed polarized total-reflection X-ray absorption fine structure method to study Zn K-edge XANES of [5,10,15,20-tetrakis(4-carboxyphenyl)-porphyrinato]zinc(II) (ZnTPPC) at the air−water interface. We have used the simplest model system, zinc porphin, to simulate Zn K- and L_3-edge XANES. Previous theoretical work carried out by Carniato et al.[8] considers copper tetraazaporphyrin (CuTAP) as a simplified model for copper phthalocyanine (CuPc) in which the benzene rings of D_4h CuPc is substituted by hydrogen atoms. They have used full core hole potential (FCH) within the DFT to calculate Cu L X-ray absorption spectrum of copper phthalocyanine. We have used a $Z + 1$ approximation in our calculations in which the nuclear charge is increased by one on the absorbing atom. The $Z + 1$ approximation is analogous to the DFT (FCH). However, in addition to the ground state XANES, we were able to simulate XANES of optically excited molecules. The excited state XANES were calculated for optical excitations which promote a valence electron from the highest occupied molecular orbital (HOMO) or any other occupied valence orbital to the lowest unoccupied molecular orbital (LUMO). We have also computed the ground state XANES of Fe(II) spin crossover compound motivated by a recent experiment[34] and predicted XANES originating from its low-lying optically excited states.

II. X-ray Spectra of Porphyrins

Calculations were performed using the hybrid density functional theory (B3LYP: Becke three parameter density functional with Lee−Yang−Parr correlation functional) and the Hartree−Fock (HF) approximation, for the electronic structures of ground state and lowest core excited state ($Z + 1$approximation). The SV basis set (split valence: inner shell atomic orbitals are described by a single basis function, two basis functions are provided for each valence shell atomic orbital) was used. This basis set is optimized and takes one-fourth CPU time compared to the all electron basis set (with diffuse function added) 6-31+G(d). The first 50 excitations were calculated using time-dependent density functional theory (TDDFT) and time-dependent Hartree−Fock (TDHF) theory. All calculations were carried out using Gaussian 03. XANES spectra were obtained using the sum over states (SOS) expressions.[35,36] Given the initial (ground state) and the final states (of the lowest core excited state) of a molecule, the SOS method calculates transitions to orbitals which have a significant dipole coupling to the core orbital vacated by the X-ray transition. The practical consequence of the $Z + 1$ approximation is that we may focus solely on valence excitations in the lowest core excited-state without having to worry about calculations of the deep-core excitation.

The visible spectra of metalloporphyrins have two bands, known as the Q and B bands, originating from transitions from two nearly degenerate highest occupied molecular orbitals (HOMO and HOMO − 1) to two degenerate lowest unoccupied molecular orbitals (LUMO and LUMO + 1). TDDFT excitation energies are known to be accurate for low-energy bands whereas TDHF excitation energies are better for high-energy bands.[28]

* Corresponding author. E-mail: smukamel@uci.edu.

10.1021/jp0627022 CCC: $37.00 © 2007 American Chemical Society
Published on Web 01/17/2007

TABLE 1: Optical Spectral Data forMgP[a]

	SV			SVP			TZV		TZVP	
sym.	*E*	*f*	sym.	*E*	*f*	sym.	*E*	*f*	*E*	*f*
EU	2.39	0.0011	EU	2.37	0.0003	EU	2.38	0.0003	2.35	0.0005
EU	3.55	0.9124	EU	3.51	0.9127	EU	3.51	0.9775	3.47	0.9689
EU	3.84	0.0964	EU	3.79	0.0981	EU	3.80	0.0626	3.75	0.0585
EU	4.23	0.3400	EU	4.20	0.2655	EU	4.23	0.2663	4.19	0.2330
A2U	5.12	0.0006		5.41	0.0018					
	5.39	0.0036	EU	5.47	0.0990		5.41	0.0023	5.43	0.0013
EU	5.52	0.1082	EU	5.98	0.0038	EU	5.51	0.1064	5.47	0.1004
EU	6.08	0.0107	EU	6.28	0.1218	EU	6.03	0.0323	5.93	0.0112
EU	6.26	0.1318	EU	6.43	0.0009	EU	6.13	0.1042	6.09	0.1124
A2U	6.47	0.0009	A2U	6.53	0.0009	A2U	6.20	0.0022	6.24	0.0027
EU	6.53	0.0040	EU	6.54	0.0269	EU	6.44	0.0086	6.30	0.0197
EU	6.66	0.0222				EU	6.52	0.0237	6.43	0.0158

[a] TDDFT with B3LYP functional and four different basis sets—SV, SVP, TZV, and TZVP—was used for the calculation of excitation energies. Molecular orbital symmetry (sym.), excitation energy (*E*) in eV and oscillator strength (*f*) in arbitrary units are listed.

TABLE 2: Optical Spectral Data for MgP and ZnP[a]

	MgP					ZnP				
	SV			SVP			SV			SVP	
sym.	*E*	*f*	sym.	*E*	*f*	sym.	*E*	*f*	sym.	*E*	*f*
EU	2.00	0.0098	EU	1.89	0.0275	EU	1.96	0.0060	EU	1.83	0.0207
EU	4.08	1.5147	EU	4.06	1.4378	EU	4.06	1.5498	EU	4.03	1.4919
EU	5.43	0.1295	EU	5.38	0.1018	EU	5.35	0.1342	EU	5.29	0.1155
AU	6.21	0.0003	AU	6.30	0.0001	A2U	5.61	0.0018	A2U	5.63	0.0005
AU	6.22	0.0005	EU	6.38	0.2974						
EU	6.39	0.3267	EU	7.61	0.0904	EU	6.30	0.3383	EU	6.28	0.3051
	7.72	0.0069		7.83	0.0024		7.69	0.0076	EU	7.63	0.0802
EU	7.74	0.1023	AU	8.06	0.0045	EU	7.75	0.0869		7.81	0.0035
AU	8.02	0.0039	EU	8.15	0.0406						
AU	8.03	0.0003				A2U	8.05	0.0034	A2U	8.08	0.0034
EU	8.30	0.0257				EU	8.40	0.0430	EU	8.24	0.0538
EU	8.71	0.0133				EU	8.77	0.0221	EU	8.79	0.0016
EU	9.03	0.2568				EU	9.05	0.2339	EU	9.01	0.2456

[a] TDHF with two different basis sets—SV and SVP—has been used for calculation of excitation energies. Molecular orbital symmetry (sym.), excitation energy (*E*) in eV, and oscillator strength (*f*) in arbitrary units are listed.

TABLE 3: Optical Spectral Data for ZnP[a]

	SV			SVP			TZV			TZVP	
sym.	*E*	*f*	sym.	*E*	*f*	sym.	*E*	*f*	sym.	*E*	*f*
EU	2.41	0.0001	EU	2.41	0.0021	EU	2.42	0.0001	EU	2.39	0.0026
EU	3.55	0.9547	EU	3.52	0.9429	EU	3.52	0.9923	EU	3.47	0.9680
EU	3.93	0.0545	EU	3.87	0.0480	EU	3.90	0.0347	EU	3.84	0.0302
EU	4.29	0.2548	EU	4.28	0.1775	EU	4.30	0.1954	EU	4.26	0.1600
AU	5.34	0.0002									
EU	5.53	0.1047				EU	5.50	0.1038	AU	5.44	0.0004
	5.63	0.0035					5.67	0.0020	EU	5.45	0.0957
EU	6.10	0.0329				EU	6.03	0.0965		5.66	0.0009
EU	6.20	0.1022				EU	6.11	0.0367	EU	5.96	0.0254
AU	6.46	0.0011				AU	6.21	0.0026	EU	6.05	0.0841
EU	6.48	0.0005				EU	6.34	0.0154	EU	6.20	0.0239
EU	6.56	0.0213				EU	6.48	0.0120	AU	6.26	0.0036

[a] TDDFT with B3LYP functional and four different basis sets—SV, SVP, TZV, and TZVP—was used for the calculation of excitation energies. Molecular orbital symmetry (sym.), excitation energy (*E*) in eV, and oscillator strength (*f*) in arbitrary units are listed.

We therefore used both techniques to calculate XANES of optically excited states. Table 1 and Table 3 compare the calculated optical excitation energies of MgP and ZnP respectively with different basis sets using TDDFT. The basis sets used were SV (described above), SVP (SV basis set with polarization function added), TZV (triple-ζ valence basis), and TZVP (triple-ζ valence basis with polarization function added). Table 2 compares TDHF excitation energies for both MgP and ZnP. In Table 4, we show optical excitation energies of ZnP taken from refs 27 and 28, The effects of basis set on optical excitation energies and oscillator strength of MgP and ZnP, examined by adding polarization functions and/or diffuse functions and using larger basis set have been found to be small. Unless otherwise stated, all calculations were performed using the SV basis set. The square planar structure of the simplest Mg (Zn) porphyrin is shown in Figure 1a. Geometry optimization was performed using B3LYP with a 6-31+G(d) basis. The computed spectra were convoluted with a Lorentzian function.

A. Mg Porphyrin. Figure 2 shows the Mg K-edge XANES of MgP in the ground and excited states, computed using TDDFT (bottom left panel) and TDHF (bottom right panel). The optical spectra are shown in the top panels. For the excited state XANES calculations, we have selected optical transitions which promote a valence electron from HOMO or any other

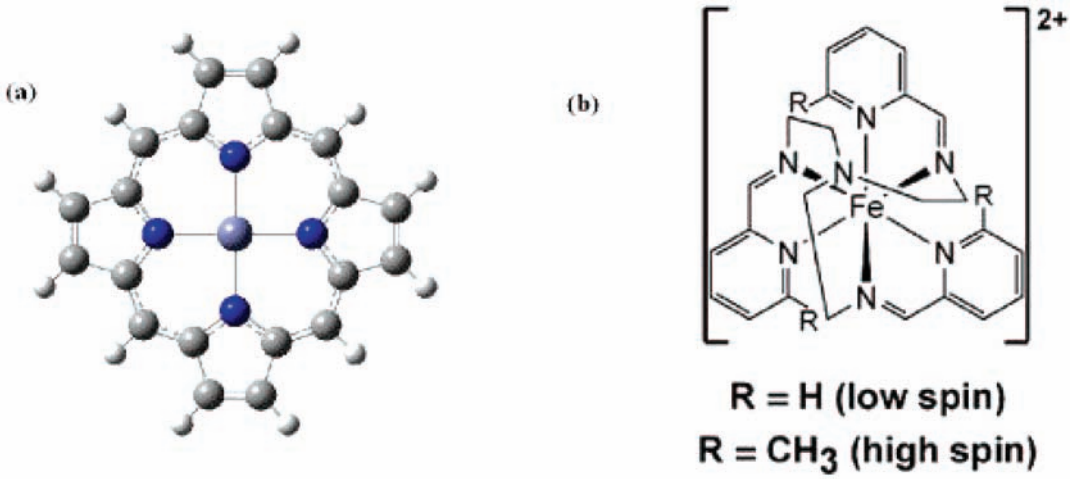

Figure 1. (a) Square planar structure of porphyrin. The central metal atom is either Mg or Zn. (b) Structure of the cation in $[Fe(tren(py)_3)](PF_6)_2$. Reprinted with permission from ref 34. Copyright 2006 American Chemical Society.

TABLE 4: Optical Spectra of ZnP Taken from References 27 and 28[a]

	6-31G(d)		6-31+G(d)		6-311+G(d)		experiment	
symmetry	*E* (eV)	*f*	*E* (eV)	*f*	*E* (eV)	*f*	*E* (eV)	*f*
EU	2.44	0.002	2.41	0.002	2.40	0.002	2.18	0.005
EU	3.54	0.889	3.49	0.960	3.48	0.949	3.13	0.98
EU	3.84	0.052	3.81	0.039	3.80	0.039	3.35	
EU	4.29	0.175	4.26	0.174	4.25	0.172	4.07	0.2
EU	5.49	0.076	5.49	0.089	5.47	0.089	5.18	0.1
A2U	5.50	0.007	5.57	0.004	5.54	0.003		
A2U	5.66	0.001	5.64	0.001	5.64	0.009		
EU	6.04	0.005	5.98	0.057			5.50	0.1
EU	6.40	0.023						

[a]All calculations were performed within TDDFT, and three different basis sets—6-31G(d), 6-31+G(d), and 6-311+G(d)—were used. Experimental data were taken in CH_3OH.

occupied valence orbital to the LUMO (indicated by arrows in the top two panels). In the ground state XANES calculated using TDDFT, three strong transitions are seen at 1306.26, 1309.37, and 1309.40 eV. The strong peak (at 1306.26 eV) corresponds to the excitation 87 → 90 of the lowest core excited-state which has maximum overlap with orbital 107 (A_{2u}) of the core filled state. Orbital 107 is a strong mixture of $2p_z$ character of N, C; and $3p_z$ has the character of Mg. The other peak is described by two close transitions at 1309.37 and 1309.40 eV corresponding to excitation 87 → 97 of the lowest core excited-state which has maximum overlap with orbital 97 (E_u), and excitation 87 → 98 of the lowest core excited-state which has maximum overlap with orbital 96 (E_u) of the core filled state (orbitals 96 and 97 are degenerate). Orbital 96 is a mixture of 2s, $2p_y$ character of N; 2s, $2p_x$, $2p_y$ character of C; and $3p_y$ character of Mg. Orbital 97 is a mixture of 2s, $2p_x$ character of N; 2s, $2p_x$, $2p_y$ character of C; and $3p_x$ character of Mg. Orbitals 97 and 107 are primarily located on the ligands (see first column of Figure 6). The Mg K-edge XANES of MgP is therefore characterized by transitions: 1s → $3p_z$, 1s → $3p_y$, and 1s → $3p_x$ of Mg.

In the excited state XANES (TDDFT) at 2.39 eV (the optical transition is not visible in the top left panel of Figure 2 due to weak oscillator strength), the weak peak is given by two transitions at 1302.14 and 1304.22 eV from core (A_{1g} symmetry) to the orbital 85 (HOMO − 1 with A_{1u} symmetry) and 86 (HOMO with A_{2u} symmetry) where an optical hole was created. Orbital 85 has strong $2p_z$ character of C, whereas orbital 86 has a mixture of $2p_z$ character of N, C, and $3p_z$ has the character of Mg (see first column of Figure 3). The main peak is slightly blue-shifted compared to the ground state XANES and can be described by three closely spaced transitions at 1306.29, 1306.34, and 1306.45 eV from core to orbital 107. The excited state XANES at 3.55 eV is red-shifted compared to the excited state XANES at 2.39 eV and the ground state XANES. The excited state XANES at 3.84 eV is mainly described by transitions from core to orbital 84 (where an optical hole was left behind) and orbital 107. Orbital 84 (HOMO − 2 with B_{2u} symmetry) is a mixture of $2p_z$ character of C and N, and is located around ligand (first column of Figure 5). Similarly the excited state XANES at 4.23 eV is described by transitions from core to orbital 81 (with an optical hole) and orbital 107. Orbital 81 (HOMO − 5 with A_{2u} symmetry) is a mixture of $2p_z$ character of C, N and $3p_z$ character of Mg. Interestingly the peak at 1300.37 eV, which is primarily described by transition from core to the orbital 81 where an optical hole was created, has larger intensity than the other peak. All the molecular orbitals which participate in the ground and excited state XANES (TDDFT) are shown in the first column of Figure 5 and Figure 6. As pointed out above the XANES spectrum at an optical excitation 2.39 eV is slightly blue-shifted. This is because an optical excitation from the HOMO to LUMO increases the positive charge on the absorbing atom. Therefore, more energy is required to excite the core electron. All other excited state XANES spectra are red-shifted. This is because when an electron is removed from inner valence orbital in the optical excitation, the electrons occupying the outer valence orbitals respond to the optical hole created. The effect of this perturbation is seen in the red shift of the XANES spectra.

Additional transitions are seen when the ground state XANES is calculated using TDHF. Three strongest transitions at 1307.90, 1310.71, and 1311.08 eV correspond to the excitations 87 → 90 [maximum overlap with orbital 110 (A_{2u}) of the core filled state], 86 → 91 [maximum overlap with orbital 92 (E_u) of the core filled state], and 85 → 91 [maximum overlap with orbital 93 (E_u) of the core filled state] respectively of the lowest core excited state. Orbitals 92 and 93 are degenerate and have E_u symmetry. Orbital 92 is a strong mixture of 2s, $2p_y$ character of N, 2s, $2p_x$, $2p_y$ character of C, and $3p_y$ character of Mg. Orbital 93 is a strong mixture of 2s, $2p_x$ character of N, 2s, $2p_x$, $2p_y$ character of C, and $3p_x$ character of Mg. Whereas orbital 110 is a mixture of $2p_z$ character of N, C and $3p_z$ character of Mg. Similar to the Mg K-edge XANES of MgP computed using TDDFT, XANES computed using TDHF is therefore also

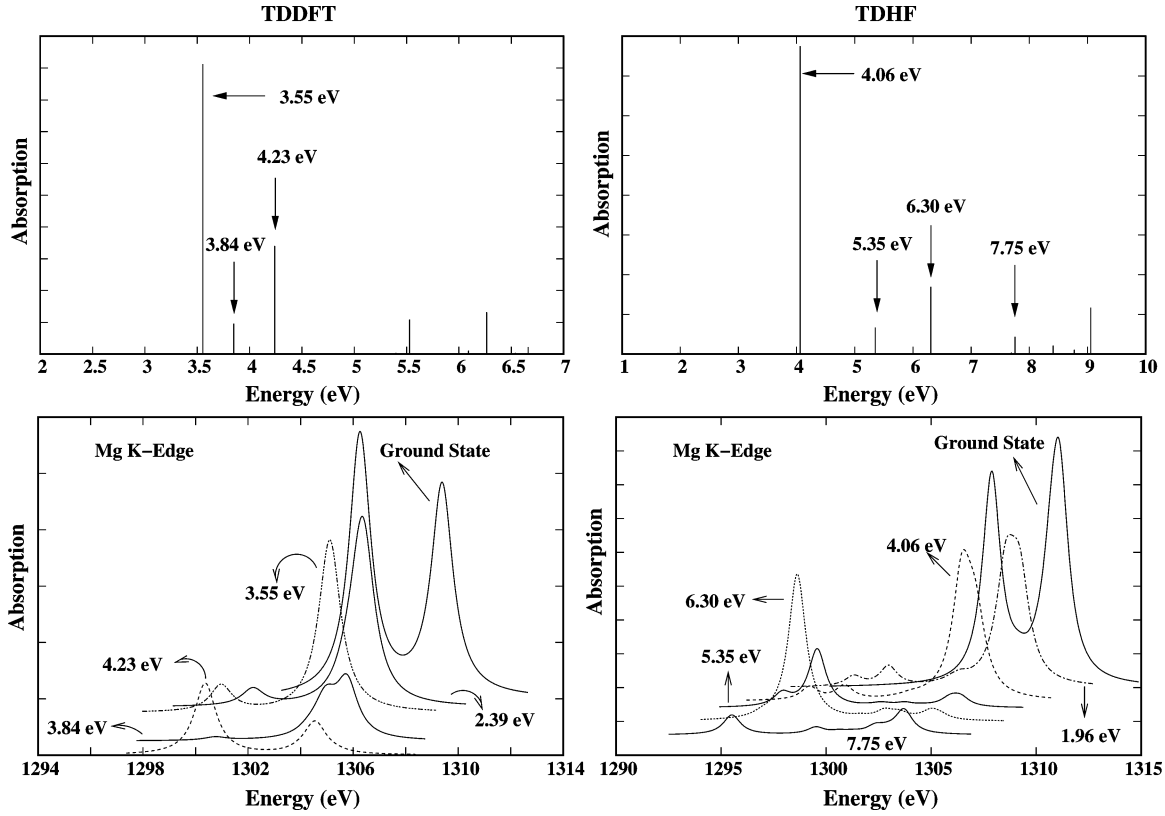

Figure 2. Mg K-edge XANES of magnesium porphyrin (MgP) simulated using TDDFT (bottom left panel) and TDHF (bottom right panel). Also shown are optical spectra computed using TDDFT (top left panel) and TDHF (top right panel). For the excited state XANES calculations, selected optical transitions are indicated by arrows on the top two panels. We select one weak transition at 2.39 eV (not visible), and three strong transitions at 3.55, 3.84, and 4.23 eV (TDDFT); one weak transition at 1.96 eV (not visible), and four strong transitions at 4.06, 5.35, 6.30, and 7.75 eV (TDHF). Line broadening $\Gamma = 1.0$ eV for the XANES spectra.

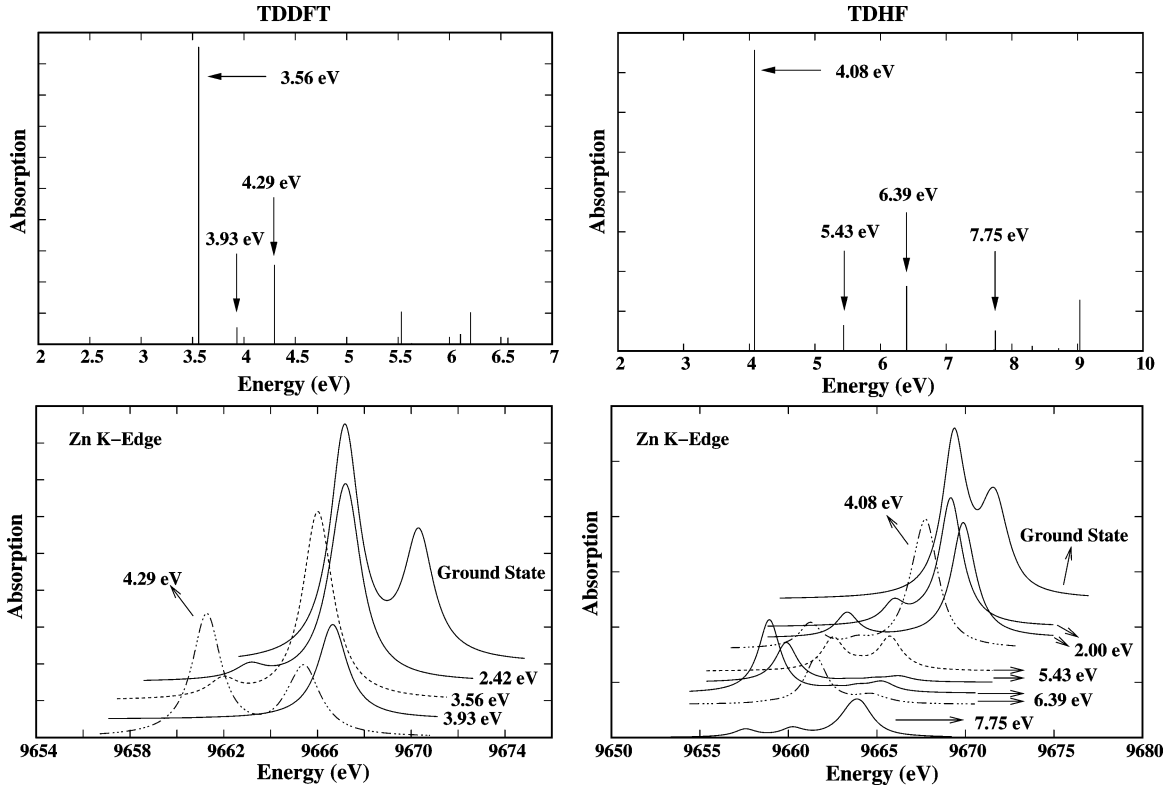

Figure 3. Zn K-edge XANES of ZnP in the ground and optically excited states, computed using TDDFT (bottom left panel) and TDHF (bottom right panel). Line broadening $\Gamma = 1.5$ eV. Top left panel (right panel) shows optical spectrum computed using TDDFT (TDHF). Selected optical transitions are indicated by arrows on the top two panels for the excited state XANES calculations. From the optical spectrum of TDDFT calculation, one weak transition at 2.42 eV (not visible), and three strong transitions at 3.56, 3.93, and 4.29 eV are selected. From the optical spectrum of TDHF calculation, one weak transition at 2.00 eV (not visible), and four strong transitions at 4.08, 5.43, 6.39, and 7.75 eV are selected.

TABLE 5: Tabulated Transitions in the Mg K-edge X-ray Absorption Spectra of MgP in the Ground and Optically Excited States[a]

E (eV)	MO	symmetry	atomic character(s)
	ground state (TDDFT)		
1306.26	107 (LUMO + 20)	A_{2u}	N, C, $2p_z$; Mg, $3p_z$
1309.37	97 (LUMO + 10)	E_u	N, 2s, $2p_x$; C, 2s, $2p_x$, $2p_y$; Mg, $3p_x$
1309.40	96 (LUMO + 9)	E_u	N, 2s, $2p_y$; C, 2s, $2p_x$, $2p_y$; Mg, $3p_y$
	excited state (2.39 eV)		
1302.14	85 (HOMO − 1)	A_{1u}	C, $2p_z$
1304.22	86 (HOMO)	A_{2u}	N, C, $2p_z$; Mg, $3p_z$
1306.29, 1306.34, 1306.45	107 (LUMO + 20)	A_{2u}	N, C, $2p_z$; Mg, $3p_z$
	ground state (TDHF)		
1307.90	110 (LUMO + 23)	A_{2u}	N, C, $2p_z$; Mg, $3p_z$
1310.71	92 (LUMO + 5)	E_u	N, 2s, $2p_y$; C, 2s, $2p_x$, $2p_y$; Mg, $3p_y$
1311.08	93 (LUMO + 6)	E_u	N, 2s, $2p_x$; C, 2s, $2p_x$, $2p_y$; Mg, $3p_x$
	excited state (1.96 eV)		
1301.31	85 (HOMO − 1)	A_{2u}	N, C, $2p_z$; Mg, $3p_z$
1302.97	86 (HOMO)	A_{1u}	C, $2p_z$
1308.14	85 (HOMO − 1)	A_{2u}	N, C, $2p_z$; Mg, $3p_z$
1308.55	86 (HOMO)	A_{1u}	C, $2p_z$
1308.90	90 (LUMO + 3)	B_{1u}	C, $2p_z$
1309.21	94 (LUMO + 7)	B_{2u}	N, $2p_x$, $2p_y$; C, 2s, $2p_x$, $2p_y$
1309.35	110 (LUMO + 23)	A_{2u}	N, C, $2p_z$; Mg, $3p_z$
	excited state (5.35 eV)		
1297.92	81 (HOMO − 5)	A_{2u}	N, C, $2p_z$; Mg, $3p_z$
1299.58	86 (HOMO)	A_{1u}	C, $2p_z$
1305.95	94 (LUMO + 7)	B_{2u}	N, $2p_x$, $2p_y$; C, 2s, $2p_x$, $2p_y$
1306.41	110 (LUMO + 23)	A_{2u}	N, C, $2p_z$; Mg, $3p_z$

[a]Calculations were performed within TDDFT and TDHF using SV basis.

TABLE 6: Relevant Transitions in the Zn K-edge X-ray Absorption Spectra of ZnP in the Ground and Optically Excited States[a]

E (eV)	MO	symmetry	atomic character(s)
	ground state (TDDFT)		
9667.16	116 (LUMO + 20)	A_u	N, C, $2p_z$; Zn, $4p_z$
9670.31	105 (LUMO + 19)	E_u	N, C, 2s, $2p_x$, $2p_y$; Zn, $4p_x$, $4p_y$
9670.34	106 (LUMO + 10)	E_u	N, C, 2s, $2p_x$, $2p_y$; Zn, $4p_x$, $4p_y$
	excited state (2.42 eV)		
9663.09	94 (HOMO − 1)	A_u	N, C, $2p_z$; Zn, $4p_z$
9663.17	95 (HOMO)	A_u	N, C, $2p_z$; Zn, $4p_z$
9666.68−9667.41	116 (LUMO + 20)	A_u	N, C, $2p_z$; Zn, $4p_z$
	excited state (3.56 eV)		
9661.95	92 (HOMO − 3)	B_u	N, C, $2p_z$
9662.03	94 (HOMO − 1)	A_u	N, C, $2p_z$; Zn, $4p_z$
9666.01	116 (LUMO + 20)	A_u	N, C, $2p_z$; Zn, $4p_z$
	ground state (TDHF)		
9669.36	119 (LUMO + 23)	A_u	N, C, $2p_z$; Zn, $4p_z$
9671.29	121 (LUMO + 25)	E_u	N, C, 2s, $2p_x$, $2p_y$; Zn, $4p_x$, $4p_y$
9671.75	122 (LUMO + 26)	E_u	N, C, 2s, $2p_x$, $2p_y$; Zn, $4p_x$, $4p_y$
	excited state (2.0 eV)		
weak peak	94 (HOMO − 1)	A_u	N, C, $2p_z$; Zn, $4p_z$
strong peak	119 (LUMO + 23)	A_u	N, C, $2p_z$; Zn, $4p_z$
	excited state (4.08 eV)		
weak peak	94 (HOMO − 1)	A_u	N, C, $2p_z$; Zn, $4p_z$
strong peak	119 (LUMO + 23)	A_u	N, C, $2p_z$; Zn, $4p_z$

[a] Calculations were performed within TDDFT and TDHF using SV basis.

characterized by the following transitions: $1s \rightarrow 3p_z$, $1s \rightarrow 3p_y$, and $1s \rightarrow 3p_x$ of Mg. The peak splitting in the ground state XANES within both TDDFT and TDHF calculations is found to be 3.13 eV. However, the peak intensities are different.

In the excited state XANES (TDHF) at 1.96 eV (too weak to be visible in the top right panel of Figure 2), two weak peaks at 1301.31 and 1302.97 eV are given by transitions from core (A_{1g} symmetry) to orbitals 85 (HOMO − 1 with A_{2u} symmetry) and 86 (HOMO with A_{1u} symmetry) where an optical hole was created. Orbital 85 is a mixture of $2p_z$ character of N, C and $3p_z$ character of Mg, whereas orbital 86 has the $2p_z$ character of C. The main peak is described by five strong transitions at 1308.14, 1308.55, 1308.90, 1309.21, and 1309.35 eV from core to orbitals 85, 86, 90, 94, and 110. These molecular orbitals are shown in the second column of Figure 5 and Figure 6. The excited state XANES at 4.06 eV has the same set of transitions as in the previous case (1.96 eV). However, it is red-shifted compared to the previous one. In the excited state XANES at 5.35 eV, the peaks at 1297.92 and 1299.58 eV are mainly given by a transition from core to orbitals 81 (HOMO − 5 with A_{2u} symmetry) and orbital 86 (HOMO) where an optical hole was created. Orbital 81 is a strong mixture of $2p_z$ character of N, C;

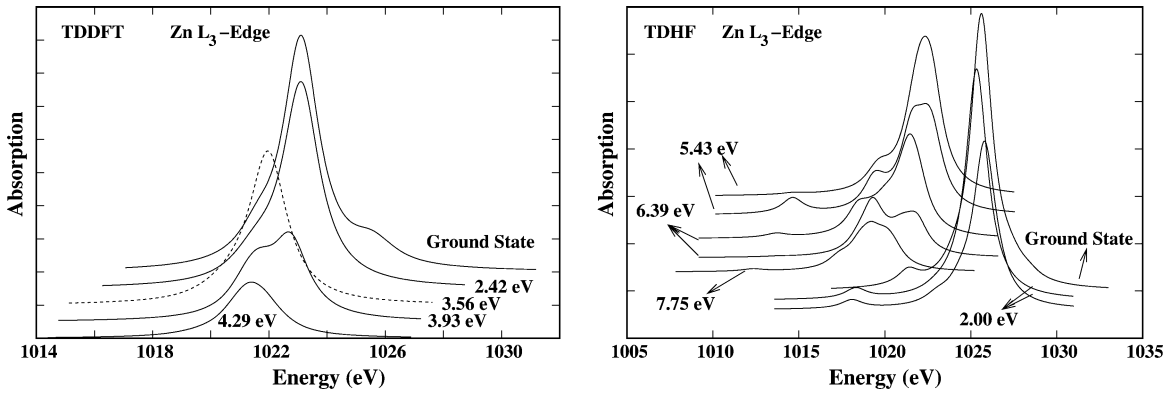

Figure 4. Zn L_3-edge XANES of ZnP in the ground and optically excited states, computed using TDDFT (left panel) and TDHF (right panel). Line broadening $\Gamma = 1.5$ eV.

and $3p_z$ character of Mg. The other peak is described by two transitions at 1305.95 and 1306.41 eV, mainly from core to orbitals 94 (B_{2u}) and 110. Orbital 94 has $2p_z$ character of N and C and is located around ligand. Similarly the excited state XANES at 6.30 eV has the same set of transitions as in the excited state XANES at 5.35 eV except that the peak at 1298.63 eV, which is primarily given by transition from core to the orbitals 81 and 84 (B_{2u}) where an optical hole was created, has larger intensity than the other peak. Orbital 84 has $2p_z$ character of N and C and is located around the ligand. Excited state XANES at 7.75 eV has a peak at 1295.52 from core to the orbital 77 (B_{1u}) with an optical hole. Orbital 77 has the $2p_z$ character of C. The effect of optical excitations on XANES is thus reflected in the change in the transition energies and intensity of transitions. Relevant X-ray transitions in both ground state and optically excited states of TDDFT and TDHF calculations are tabulated in Table 5.

B. Zn Porphyrin. Simulated Zn K-edge XANES of ZnP in the ground and excited states are shown in Figure 3: TDDFT (bottom left panel) and TDHF (bottom right panel). The optical spectra are shown in the top panels. For the excited state XANES calculations, we selected optical transitions which promote a valence electron from HOMO or any other occupied valence orbital to the LUMO and are indicated by arrows in the top two panels. In the ground state XANES of TDDFT calculation three strong transitions are seen. The first peak is described by a transition at 9667.16 eV corresponding to the excitation 96 → 100 of the lowest core excited-state which has maximum overlap with orbital 116 (A_u) of the core filled state. Orbital 116 is a strong mixture of $2p_z$ character of N, C; and $4p_z$ character of Zn. Therefore, this peak is assigned by transition: $1s \rightarrow 4p_z$ of Zn. The other peak is described by two equally intense transitions at 9670.31 and 9670.34 eV corresponding to the excitations 96 → 106 and 96 → 107 of the lowest core excited-state which have maximum overlap with orbitals 105 (E_u) and 106 (E_u) of the core filled state. Orbitals 105 and 106 are degenerate and are a strong mixture of the 2s, $2p_x$, $2p_y$ character of N, C and the $4p_x$, $4p_y$ character of Zn. This peak is therefore assigned by degenerate transitions: $1s \rightarrow 4p_x$, $1s \rightarrow 4p_y$ of Zn. Our simulated ground state XANES of ZnP may be compared with the experimental spectra of Tanida et al.[33] A complete agreement with their experimental spectra may not be expected because ours is the simplest model system.

In the excited state XANES (TDDFT) at 2.42 eV (not visible in the top left panel of Figure 3), the weak peak is given by two closely spaced transitions at 9663.09 and 9663.17 eV from core (A_g symmetry) to the orbitals 94 (HOMO − 1) and 95 (HOMO) where an optical hole was created in the excitation. Orbitals 94 and 95 have A_u symmetry and are mixture of the $2p_z$ character of N, C and the $4p_z$ character of Zn. The strong peak is described by five transitions between 9666.68 and 9667.41 eV mainly from the core to the orbital 116. The strong peak in the excited state XANES is essentially unchanged in energy compared to the strong peak in the ground state XANES. The excited state XANES at 3.56 eV, however, is red-shifted. The strong peak in this is mainly described by a transition at 9666.01 eV from core to orbital 116. The weak peak is described by two closely spaced transitions at 9661.95 and 9662.03 eV from core to orbitals 92 and 94 (with an optical hole). Orbital 92 has B_u symmetry and is a mixture of $2p_z$ character of N and C. Similarly the excited state XANES at 3.93 eV is given by one weak peak at 9661.66 eV (transition from core to orbital 92 with an optical hole) and strong peak at 9666.65 eV (transition from core to orbital 116). Interestingly in the excited state XANES at 4.29 eV, the strong peak at 9661.29 eV, which is primarily described by transition from core to the orbital 89 where an optical hole was created, has larger intensity than the other peak. Orbital 89 has A_u symmetry and is a mixture of $2p_z$ character of N, C; and $4p_z$ character of Zn. The effect of optical excitations on XANES is reflected in the change in the transition energies and intensity of transitions and is suggestive of changes in the molecular geometry and charge density around the absorbing atom. All the molecular orbitals which participate in the ground and excited state XANES (TDDFT) are shown in the third column of Figures 5 and 6.

In the XANES of TDHF calculations, three strongest transitions: at 9669.36, 9671.29, and 9671.75 eV correspond to the excitations 96 → 98 (maximum overlap with orbital 119 (A_u) of the core filled state), 95 → 100 (maximum overlap with orbital 121 (E_u) of the core filled state), and 94 → 100 (maximum overlap with orbitals 122 (E_u) and 101 (E_u) of the core filled state) respectively of the lowest core excited state. Orbitals 121 and 122 are degenerate and are strong mixture of the 2s, $2p_x$, $2p_y$ character of N, C and the $4p_x$, $4p_y$ character of Zn. Similarly orbital 101 is a strong mixture of the 2s, $2p_x$, $2p_y$ character of N, C and the $4p_x$, $4p_y$ character of Zn. Orbital 119 on the other hand is a mixture of the $2p_z$ character of N, C and the $4p_z$ character of Zn. Similar to the Zn K-edge XANES of ZnP computed using TDDFT, XANES computed using TDHF is therefore characterized by the following transitions: $1s \rightarrow 4p_z$, $1s \rightarrow 4p_x$, and $1s \rightarrow 4p_y$ of Zn. The peak splittings in the ground state XANES within TDDFT (3.14 eV) and TDHF (2.25 eV) calculations are found to be different. However, the intensity ratio of the peaks are similar in both cases.

The XANES spectra of the two degenerate optically excited states at 2.0 eV are different. In both the spectra the weak peak results from a transition from core (A_g symmetry) to orbital 94 (HOMO − 1) where an optical hole was left behind in the

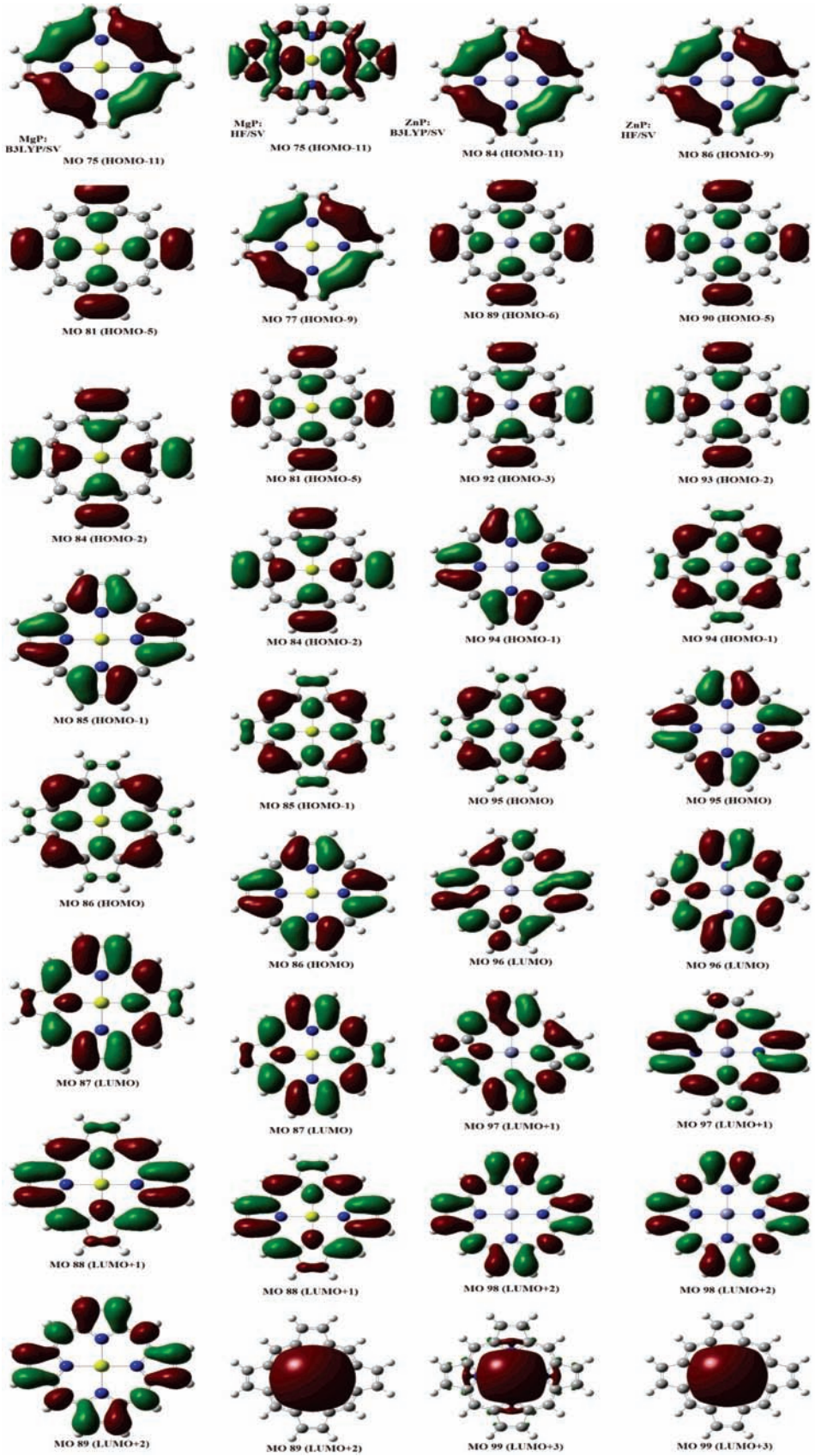

Figure 5. Molecular orbitals of MgP and ZnP. First (second) column from left: molecular orbitals of MgP obtained within B3LYP(HF)/SV. Third (fourth) column from left: molecular orbitals of ZnP obtained using B3LYP(HF)/SV.

excitation. Whereas the strong peak in both the spectra is mainly described by a transition from core to orbital 119. The strong peak is slightly red-shifted in one, but it is blue-shifted in the other compared to the strong peak of the ground state XANES. In the excited state XANES at 4.08 eV, the weak peak is given by transition from core to orbital 94 (HOMO − 1) where an optical hole was created. The strong peak is mainly described by a transition from core to orbital 119. It is red-shifted

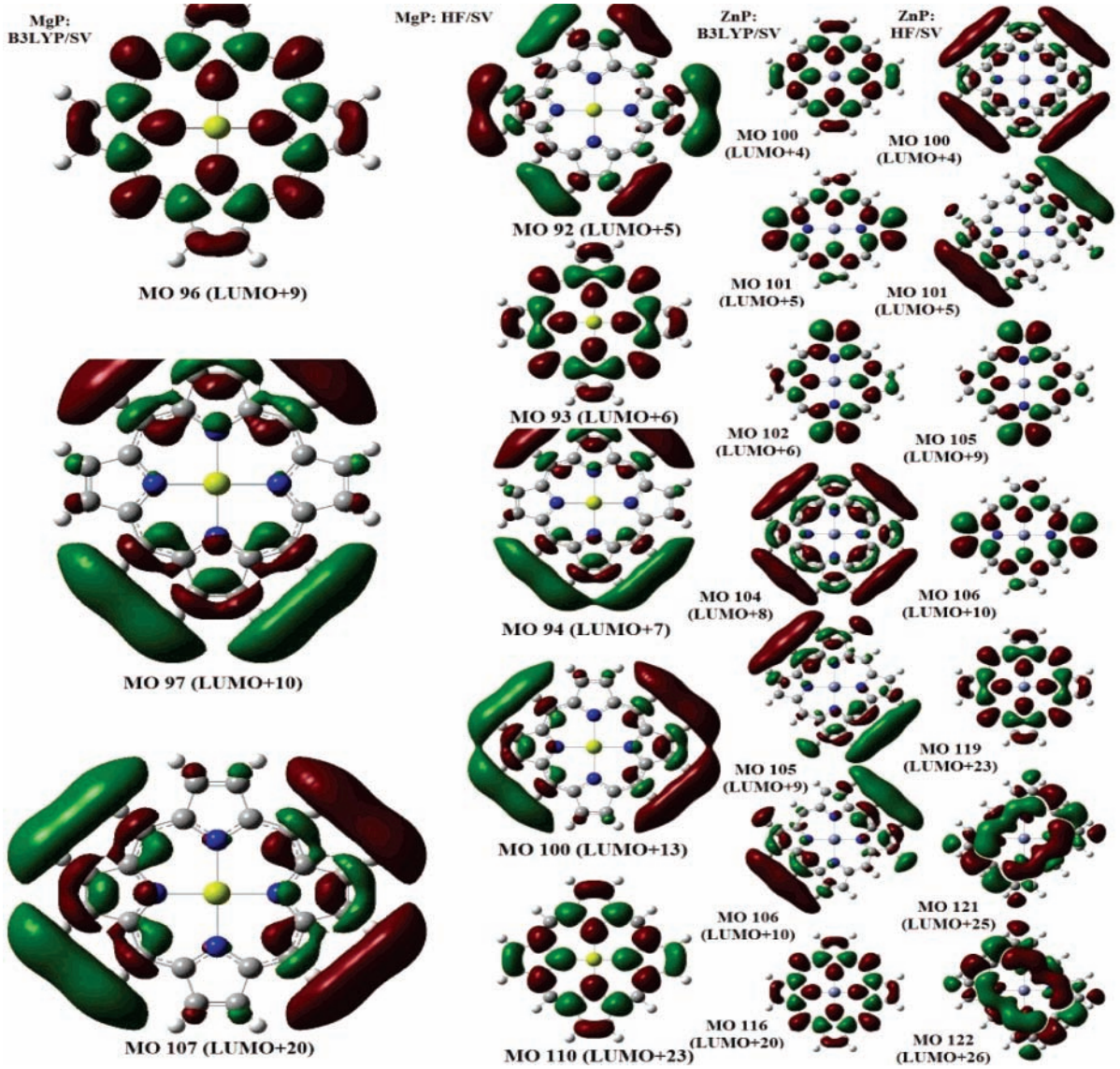

Figure 6. Molecular orbitals of MgP and ZnP. First (second) column from left: molecular orbitals of MgP obtained within B3LYP(HF)/SV. Third (fourth) column from left: molecular orbitals of ZnP obtained using B3LYP(HF)/SV.

compared to the strong peak of the ground state XANES. Orbital 94 has A_u symmetry and is a strong mixture of the $2p_z$ character of N, C and the $4p_z$ character of Zn. In the XANES spectra of two degenerate optically excited states at 5.43 eV, the preedge peak corresponding to transition from core to orbital 90 has a larger intensity than the other peak. Similarly in the XANES spectra of two degenerate optically excited states at 6.39 eV, the preedge peak corresponding to transition from core to orbital 90 has a larger intensity than the other peak. Orbital 90 has A_u symmetry and is a mixture of the $2p_z$ character of N, C and the $4p_z$ character of Zn. The variation in transition energies and intensities in the excited state XANES implies a variation in the geometry of the molecule and the charge density in the molecule around the absorbing atom upon optical excitations. All the molecular orbitals which participate in the ground and excited state XANES (TDHF) are shown in the fourth column of Figures 5 and 6. Relevant X-ray transitions in both ground state and optically excited states of TDDFT and TDHF calculations are also tabulated in Table 6.

Figure 4 is for L_3-edge XANES of ZnP in the ground and excited states computed within TDDFT (left panel) and TDHF (right panel). In the ground state XANES of left panel, two strong transitions at 1021.56 and 1021.64 eV are seen from core (A_u and E_u symmetries) to LUMO and LUMO + 1 (two lowest unoccupied molecular orbitals: 96 (LUMO), 97 (LUMO + 1) are degenerate and have E_g symmetry.). Orbitals 96 and 97 are a mixture of the $4d_{xz}$, $4d_{yz}$ atomic orbitals of Zn and the $2p_z$ character of N and C. The strongest transition at 1023.10 eV results from core to the LUMO + 3 (orbital 99 with A_g symmetry), which is a strong mixture of the $4d_{xy}$ atomic orbital of Zn and the 2s, $2p_x$, $2p_y$ character of N, C. Transition at 1025.35 eV is from core to orbital 102 with E_g symmetry. Two degenerate transitions at 1025.58 eV correspond to transition from core to degenerate orbitals 101, 102 (E_g). Orbitals 101 and 102 are mixtures of the $4d_{xz}$, $4d_{yz}$ character of Zn and the $2p_z$ character of N, C. Transition at 1026.11 eV is from core to orbital 104 with A_g symmetry, which is a strong mixture of $4d_{xy}$ atomic orbital of Zn and 2s, $2p_x$, $2p_y$ character of N, C. Most of the transitions (nearly 12) between 1025.01 and 1026.04 eV which contribute to the spectrum arise from core to either orbital 101 or orbital 102.

For the excited state L_3-edge XANES (TDDFT), the selected optical transitions are indicated by arrows in Figure 3 (left panel). The excited state XANES at 2.42 eV is described by transitions from core to orbitals 96 and 97 between 1020.76 and 1022.60 eV (total of seven transitions). Two nearly

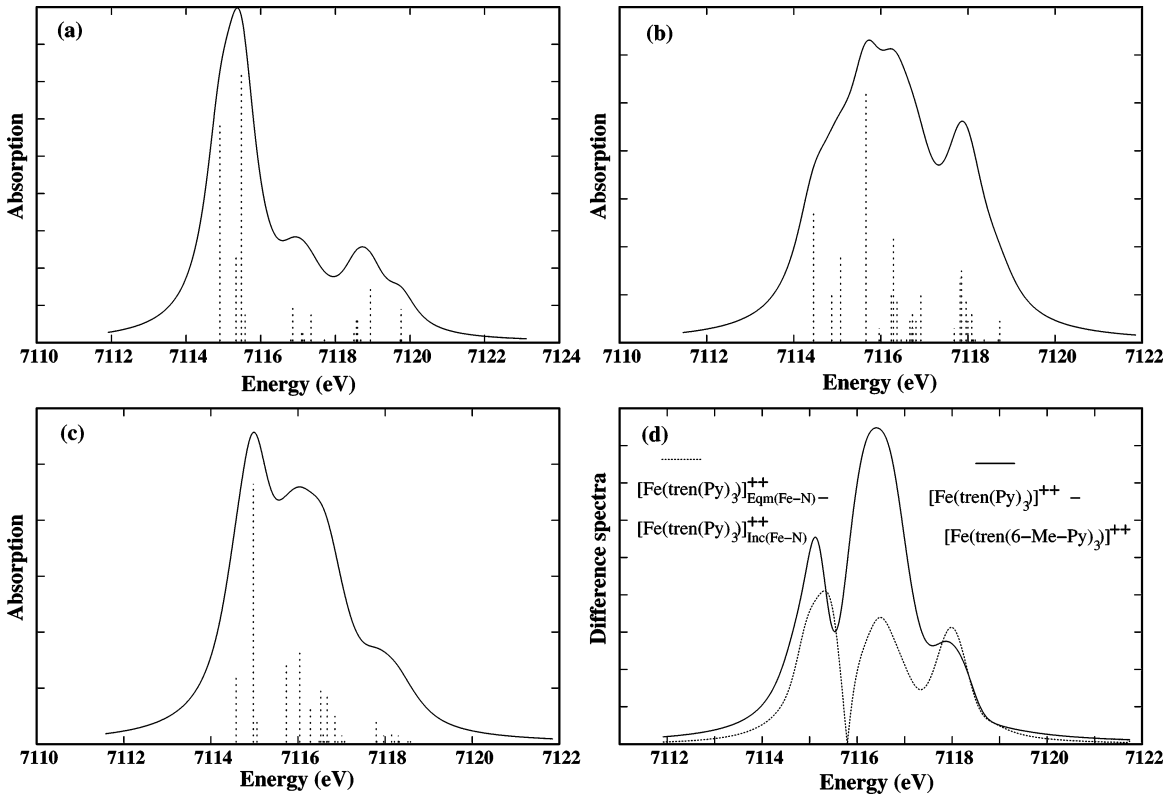

Figure 7. Simulated Fe K-edge XANES of (a) low spin $[Fe(tren(py)_3)]^{2+}$, (b) high spin $[Fe(tren(py)_3)]^{2+}$, and (c) high spin analogue, $[Fe(tren(6\text{-Me-py})_3)]^{2+}$, and (d) difference spectra between high and low spin states. Dashed line in (d) shows the difference spectrum of $[Fe(tren(py)_3)]^{2+}$ with equilibrium and increased bond lengths (low and high spin states). Solid line is for the difference spectrum of $[Fe(tren(py)_3)]^{2+}$ with equilibrium bond length (low spin) and $[Fe(tren(6\text{-Me-py})_3)]^{2+}$ (high spin analogue), computed using TDDFT. Line broadening $\Gamma = 1.0$ eV.

TABLE 7: Relevant Transitions in the Zn L_3-Edge X-ray Absorption Spectra of ZnP in the Ground and Optically Excited States[a]

E (eV)	MO	symmetry	atomic character(s)
	ground state (TDDFT)		
1021.56	96 (LUMO)	E_g	N, C, $2p_z$; Zn, $4d_{xz}$, $4d_{yz}$
1021.64	97 (LUMO + 1)	E_g	N, C, $2p_z$; Zn, $4d_{xz}$, $4d_{yz}$
1023.10	99 (LUMO + 3)	A_g	N, C, 2s, $2p_x$, $2p_y$; Zn, $4d_{xy}$
1025.35	102 (LUMO + 6)	E_g	N, C, $2p_z$; Zn, $4d_{xz}$, $4d_{yz}$
1026.11	104 (LUMO + 8)	A_g	N, C, 2s, $2p_x$,$2p_y$; Zn, $4d_{xy}$
	excited state (2.42 eV)		
1020.76−1022.60	96 (LUMO), 97 (LUMO + 1)	E_g	N, C, $2p_z$; Zn, $4d_{xz}$, $4d_{yz}$
1022.76	99 (LUMO + 3)	A_g	N, C, 2s, $2p_x$, $2p_y$; Zn, $4d_{xy}$
1022.78	97 (LUMO + 1)	E_g	N, C, $2p_z$; Zn, $4d_{xz}$, $4d_{yz}$
1023.08, 1023.17	99 (LUMO + 3)	A_g	N, C, 2s, $2p_x$, $2p_y$; Zn, $4d_{xy}$
	excited state (3.93 eV)		
1019.25−1022.22	96 (LUMO), 97 (LUMO + 1)	E_g	N, C, $2p_z$; Zn, $4d_{xz}$, $4d_{yz}$
1022.75	99 (LUMO + 3)	A_g	N, C, 2s, $2p_x$, $2p_y$; Zn, $4d_{xy}$
	ground state (TDHF)		
1021.37	96 (LUMO)	E_g	N, C, $2p_z$; Zn, $4d_{xz}$, $4d_{yz}$
1024.01	97 (LUMO + 1)	E_g	N, C, $2p_z$; Zn, $4d_{xz}$, $4d_{yz}$
1025.62	99 (LUMO + 3)	A_g	N, C, 2s, $2p_x$, $2p_y$; Zn, $4d_{xy}$
1026.60−1028.51	105 (LUMO + 9), 106 (LUMO + 10)	E_g	N, C, $2p_z$; Zn, $4d_{xz}$, $4d_{yz}$
	excited state (2.0 eV)		
1018.33	96 (LUMO), 97 (LUMO + 1)	E_g	N, C, $2p_z$; Zn, $4d_{xz}$, $4d_{yz}$
1025.34	99 (LUMO + 3)	A_g	N, C, 2s, $2p_x$, $2p_y$; Zn, $4d_{xy}$

[a] Calculations were performed within TDDFT and TDHF using SV basis.

degenerate transitions at 1022.76 and 1022.78 eV are mainly from core to orbitals 99 and 97, respectively. The main peak is described by the two strongest transitions at 1023.08 and 1023.17 eV from core to orbital 99. The excited state XANES at 3.56 eV has the same set of transitions as described above except that it is red-shifted. Similarly the excited state XANES at 3.93 eV is described by transitions from core to orbitals 96 and 97 between 1019.25 and 1022.22 eV (total 11 transitions). The strongest peak corresponds to transitions at 1022.75 eV and is mainly from core to orbital 99. In the excited state XANES at 4.29 eV, the spectrum between 1018.89 and 1020.91 is described by transitions from core to orbital 96 and 97. Two degenerate and strong transitions at 1021.29 eV are from core to orbital 99 and orbitals 96, 97. Two more strong and nearly degenerate transitions at 1021.82 and 1021.85 eV are from core to orbitals 96, 97. Another strong transition at 1022.39 eV is

mainly described by core to orbital 99. The L_3-edge XANES of ZnP in the ground and optically excited states are thus described by transitions from core to orbitals 96, 97, 99, 101, 102, and 104. These molecular orbitals, essentially a mixture of Zn 4d and N, C 2s, 2p, are shown in the third column of Figures 5 and 6.

In the ground state XANES of right panel (TDHF calculations), two strong transitions at 1021.37 and 1024.01 eV are seen from core (A_u and E_u symmetries) to LUMO (orbital 96) and LUMO + 1 (orbital 97). These orbitals are degenerate and have E_g symmetry. Similar to the TDDFT, orbitals 96 and 97 of TDHF are mixture of $4d_{xz}$, $4d_{yz}$ character of Zn and $2p_z$ character of N and C. The strongest transition at 1025.62 eV results from core to the LUMO + 3 (orbital 99 with A_g symmetry), which contribute to the strong peak. As in the TDDFT orbital 99 of TDHF calculation is a strong mixture of the $4d_{xy}$ atomic orbital of Zn and the 2s, $2p_x$, $2p_y$ character of N, C. Six relatively weak transitions between 1026.60 and 1028.51 eV are seen from core to two degenerate orbitals 105 and 106 (E_g). Orbitals 105 and 106 are mixtures of $4d_{xz}$, $4d_{yz}$ character of Zn and $2p_z$ character of N, C. Many other small amplitude transitions contribute to the spectrum. They are either from core to degenerate orbitals 96, 97 or from core to degenerate orbitals 105, 106.

For the excited state L_3-edge XANES of TDHF calculations, selected optical transitions are indicated by arrows in Figure 3 (right panel). Two excited state XANES corresponding to degenerate initial optical excitations from HOMO and HOMO − 1 to LUMO (2.0 eV) are depicted. In the upper spectrum, the weak peak is described by a transition at 1018.33 eV from core to degenerate orbitals 96 and 97. The strong peak is primarily described by transition from core to orbital 99 at 1025.34 eV. However, this peak is red-shifted compared to the ground state XANES. In the lower spectrum, the weak peak is described by a transition at 1018.07 eV from core to degenerate orbitals 96 and 97. The strong peak is primarily described by transition from core to orbital 99 at 1025.80 eV. This peak is blue-shifted compared to the ground state XANES. Many small amplitude transitions contribute to the spectrum. They are either from core to degenerate orbitals 96, 97 or from core to degenerate orbitals 105, 106. The excited state XANES at doubly degenerate optical excitations, 5.43 and 6.39 eV, and the excited state XANES at 7.75 eV are described by transitions from core to degenerate orbitals 96, 97 and from core to degenerate orbitals 105, 106. These molecular orbitals are essentially mixture of Zn 4d and N, C 2s,2p. The variation in transition intensities in the excited state XANES implies variation in the charge density in the molecule around the absorbing atom. All the molecular orbitals which participate in the ground and excited state XANES (TDHF) are shown in the fourth column of Figures 5 and 6. X-ray transitions in both ground state and optically excited states of TDDFT and TDHF calculations are also tabulated in Table 7.

III. X-ray Spectra of a Iron(II) Spin Crossover Compound

The multidentate ligand structure of cation in $[Fe(tren(py)_3)](PF_6)_2$ is shown in Figure 1b (reprinted from ref 34). This compound has a low spin (singlet) ground state. The addition of methyl groups results in the high spin (quintet) ground state and provides the means to tune the physical properties of the Fe(II) compound.

Khalil et al.[34] have recently reported steady state and time-resolved X-ray absorption spectra (XAS) measurements on the iron K-edge of $[Fe(tren(py)_3)](PF_6)_2$, a spin crossover complex dissolved in acetonitrile solution. They also measured the steady-state XAS of its high spin analogue, $[Fe(tren(6\text{-}Me\text{-}py)_3)](PF_6)_2$. In the time-resolved study, 100 fs, 400 nm pump pulses initiate a charge-transfer transition in the low spin complex ($^1A_1 \rightarrow {}^1$MLCT). Subsequently within ~300 fs the complex relaxes to high spin $^5T_2$ term as its lowest excited-state, which has a longer lifetime (~60 ns). The transient X-ray absorption difference spectrum of the complex (between its low and high spin states) was recorded 330 ps after the optical excitation. The difference of the static X-ray absorption measurements of low spin parent complex and high spin analogue was found to be identical to the transient X-ray absorption difference spectrum of $[Fe(tren(py)_3)](PF_6)_2$. This implies that the spectroscopic features of photoinduced high spin state $^5T_2$ of the parent compound $[Fe(tren(py)_3)](PF_6)_2$ is identical to that of the high spin analogue, $[Fe(tren(6\text{-}Me\text{-}py)_3)](PF_6)_2$[34].

We have simulated XANES of $[Fe(tren(py)_3)]^{2+}$ ([iron tris(*N*-(2-pyridylmethyl)-2-iminoethyl)amine]$^{2+}$) in its ground state (low spin) and excited state (high spin). The structure was obtained from X-ray crystallography data.[37] Geometry optimization of both low and high spin states was performed using B3LYP with 3-21G basis. The average Fe−N bond length was increased by 0.21 Å in the high spin state (quintet). Note that the high spin excited-state does not involve an optical hole in the valence. The average Fe−N bond length of low (high) spin $[Fe(tren(py)_3)]^{2+}$ was found to be 1.95 (2.16) ± 0.01 Å, in good agreement with experiment [1.96 (2.17) ± 0.01 Å].[34] The replacement of hydrogen atoms ortho to the pyridyl nitrogens with methyl groups in the ground state of the parent compound (singlet) results in high spin state (quintet). Geometry of this high spin analogue, $[Fe(tren(6\text{-}Me\text{-}py)_3)]^{2+}$ was optimized using B3LYP with 3-21G basis. The average Fe−N bond length was found to be 2.18 ± 0.01 Å, in good agreement with the experiment (2.19 ± 0.01 Å).[34] This resulting high spin analogue mimics similar spectral features in its ground state XANES as the XANES of high spin excited state (quintet) of the parent compound.[34] We have simulated XANES of this high spin analogue and compared the difference spectra of low and high spin states. Figure 7a shows Fe K-edge XANES of low spin $[Fe(tren(py)_3)]^{2+}$. Ground state electronic structure calculations were performed using B3LYP with 3-21G basis. Excited states were computed using TDDFT. Transitions are dominated by 1s core orbital of Fe to the unoccupied orbitals, essentially a mixture of Fe 4s, 4p and N 2p. Figure 7b is for Fe K-edge XANES of high spin $[Fe(tren(py)_3)]^{2+}$. The average Fe−N bond length is increased by ~0.21 Å. Therefore, the unoccupied states around Fe have lesser N 2p character. These are reflected in the transition energies and intensity of transitions. Fe K-edge XANES of high spin analogue, $[Fe(tren(6\text{-}Me\text{-}py)_3)]^{2+}$ is shown in Figure 7c. The spectrum shown in part c should mimic similar features as spectrum b.[34] To explore this we have plotted the difference spectra of low and high spin states in Figure 7d. These results are consistent with those observed by Khalil et al.[34]

We have further studied the XANES of low lying optically excited-state of (low spin) $[Fe(tren(py)_3)]^{2+}$. The optical spectrum of this complex calculated using TDDFT with 3-21G basis is shown in Figure 8. We selected optical transitions which promote the electron from HOMO or any other occupied valence orbitals to the LUMO (indicated by arrows). A total of nine such transitions are selected: 1.71 eV, which is not visible due to weak oscillator strength, four relatively weak transitions at 1.86, 2.20, 4.53, and 5.11 eV, and four strong transitions at 2.25, 2.54, 4.44, and 4.82 eV. Computed excited state XANES

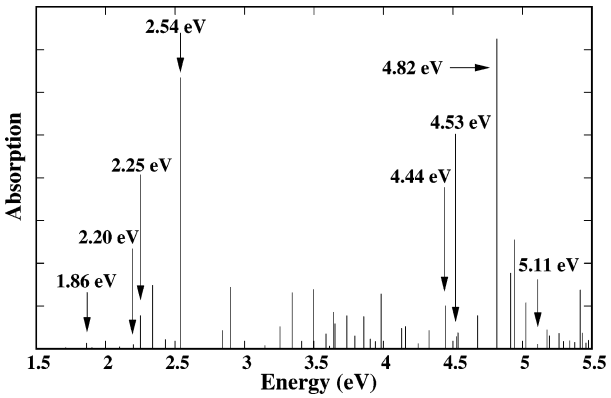

Figure 8. Optical spectrum of $Fe[tren(py)_3]^{2+}$ calculated within TDDFT. Selected optical excitations for the excited state XANES are indicated by arrows.

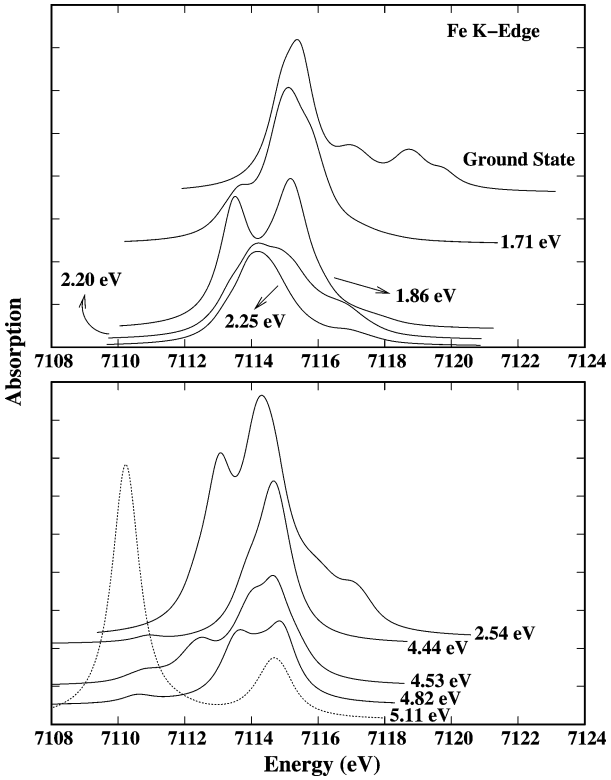

Figure 9. Fe K-edge XANES of $Fe[tren(py)_3]^{2+}$ in the ground and optically excited states, simulated using TDDFT. Line broadening $\Gamma = 1.0$ eV.

spectra along with the ground state XANES are encapsulated in Figure 9. Ground state calculations were carried out using B3LYP with 3-21G basis. Excited states were computed using TDDFT. One hundred excited states of the lowest core excited-state were computed to get as much XANES transitions as possible. Number of occupied orbitals are 122. The main peak of the ground state XANES corresponds to three strongest transitions at 7114.91, 7115.34, and 7115.48 eV and one relatively weak transition at 7115.58 eV. Transition at 7114.91 eV is given by the lowest core excited state, which gives maximum overlap with orbital 129 of core filled state. The 7115.34 and 7115.48 eV transitions are given by excitations 123 → 124 and 123 → 129 respectively of the lowest core excited state (maximum overlap with orbitals 123 and 131 respectively). 7115.58 eV transition is described by the excitation 123 → 125 of the lowest core excited state, which gives maximum overlap with orbital 124 of the core filled state. These unoccupied orbitals are essentially mixture of Fe 4s, 4p and N 2p. The second peak is described by many small amplitude transitions essentially from core to orbital 125 (at 7116.81, 7116.86 eV), orbital 126 (7117.09, 7117.13, and 7117.17 eV), orbital 127 (7117.35 eV), and orbital 128 (7117.70 eV). Similarly the third peak is given by many small amplitude transitions mainly from core to orbital 130 (five transitions between 7118.50 and 7118.68 eV) and a strong transition from core to orbital 132 at 7118.94 eV. The fourth peak is contributed by three nearly degenerate transitions at 7119.74, 7119.76, and 7119.77 eV from core to the orbital 133. The excited state XANES spectra, however, are dominated by transitions from core to the orbital, where an optical hole was created in the excitation, and from core to orbital 129. In all the excited state XANES spectra the most dominant contribution comes from transition: core → orbital 129. The effect of optical excitations on XANES is reflected in change in the transition energies and intensity of transitions. This suggests changes in the charge density and molecular geometry of the molecule around the absorbing atom upon optical excitation.

IV. Conclusions

We have calculated XANES of organometallic compounds in their ground state and low-lying optically excited states. The excited state XANES give information about changes in the conformation, charge density, and molecular geometry of the molecule upon optical excitation. This is reflected in change in the transition energies and intensity of transitions. Simulated excited state XANES spectra may be used to mimic optical pump X-ray probe experiments, whereby an optical pump excites the valence electrons which are then monitored by the X-ray probe. To that end they need to be combined with time-resolved excited-state dynamics of molecules in gas phase and in the liquid environment. Ultrafast X-ray sources can provide attosecond snapshots of interatomic distances and changes in the geometry and charge distribution of molecules. Dynamical processes such as vibrational excitation, bond formation and breaking, relaxation, and time-dependent solvation processes can be monitored on the fly.

Acknowledgment. We gratefully acknowledge the support from Chemical Sciences, Geosciences and Biosciences Division, Office of Basic Energy Sciences, Office of Science, U.S. Department of Energy.

References and Notes

(1) Shiro, Y.; Sato, F.; Suzuki, T.; Iizuka, T.; Matsushita, T.; Oyanagi, H. *J. Am. Chem. Soc.* **1990**, *112*, 2921.
(2) Longa, S. D.; Arcovito, A.; Girasole, M.; Hazemann, J. L.; Benfatto, M. *Phys. Rev. Lett.* **2001**, *87*, 155501.
(3) Baldwin, K. C.; Tierney, D. L.; Govindaswamy, N.; Gruff, E. S.; Kim, C.; Berg, J.; Koch, S. A.; Penner-Hahn, J. E. *J. Am. Chem. Soc.* **1998**, *120*, 8401.
(4) Kim, S.; Bae, I. T.; Sandifer, M.; Ross, P. N.; Carr, R.;Woicik, J.; Antonio, M. P.; Scherson, D. A. *J. Am. Chem. Soc.* **1991**, *113*, 9063.
(5) Carrado, K. A.; Wasserman, S. *R. Chem. Mater.* **1996**, *8*, 219.
(6) Bae, I. T.; Scherson, D. A. *J. Phys. Chem. B* **1998**, *102*, 2519.
(7) Kurmaev, E. Z.; Shamin, S. N.; Galakhov, V. R.;Moewes, A.; Otsuka, T.; Koizume, S.; Endo, K.; Katz, H. E.; Bach, M.; Neumann, M.; Ederer, D. L.; Iwami, M. *Phys. Rev. B* **2001**, *64*, 045211.
(8) Carniato, S.; Luo, Y.; Ågren, H. *Phys. Rev. B* **2001**, *63*, 085105.
(9) Kim, D.; Kirmaier, C.; Holten, D. *Chem. Phys.* **1983**, *75*, 305.
(10) Kim, D.; Holten, D. *Chem. Phys. Lett.* **1983**, *98*, 584.
(11) Chen, L. X.; Jägger, W. J. H.; Jennings, G.; Gosztola, D. J.; Munkholm, A.; Hessler, J. P. *Science* **2001**, *292*, 262.
(12) Chen, L. X. *J. Electron Spectrosc. Relat. Phenom.* **2001**, *119*, 161.
(13) Chen, L. X. *Annu. Rev. Phys. Chem.* **2005**, *56*, 221.
(14) Campbell, L.; Tanaka, S.; Mukamel, S. *Chem. Phys.* **2004**, *299*, 225.
(15) Kim, B. F.; Bohandy, J.; Jen, C. K. *J. Chem. Phys.* **1973**, *59*, 213.

(16) Gouterman, M. *The Porphyrins*; Dolphin, D., Ed.; Academic Press. Inc.: New York, 1978; Vol. III.
(17) Plleni, M.-P.; Grätzel, M. *J. Phys. Chem.* **1980**, *84*, 1822.
(18) Bohandy, J.; Kim, B. F. *J. Chem. Phys.* **1980**, *73*, 5477.
(19) Keegan, J. D.; Stolzenberg, A. M.; Lu, Y.-C.;Linder, R. E.; Barth, G.; Moscowitz, A.; Bunnenberg, E.; Djerassi, C. *J. Am. Chem. Soc.* **1982**, *104*, 4305.
(20) Rodriguez, J.; Kirmaier, C.; Holten, D. *J. Chem. Phys.* **1991**, *94*, 6020.
(21) Bhyrappa, P.; Krishnan, V. *Inorg. Chem.* **1991**, *30*, 239.
(22) Rempel, U.; Brunn, R.; von Borczyskowski, C. *SPIE* **1992**, *1921*, 122.
(23) Davis, W.; Calongne, S.; Rodriguez, J. *J. Chem. Phys.* **1995**, *102*, 716.
(24) Woller, E. K.; DiMango, S. G. *J. Org. Chem.* **1997**, *62*, 1588.
(25) Rubio, M.; Roos, B. O.; Serrano-Andres, L.; Merchan, M. *J. Chem. Phys.* **1999**, *110*, 7202.
(26) Nguyen, K. A.; Day, P. N.; Pachter, R. *J. Chem. Phys.* **1999**, *110*, 9135.
(27) Nguyen, K. A.; Pachter, R. *J. Chem. Phys.* **2001**, *114*, 10757.
(28) Nguyen, K. A.; Day, P. N.; Pachter, R.; Tretiak, S.; Chernyak, V.; Mukamel, S. *J. Phys. Chem. A* **2002**, *106*, 10285.
(29) Nguyen, K. A.; Pachter, R. *J. Chem. Phys.* **2003**, *118*, 5802.
(30) Liao, M.-S.; Scheiner, S. *J. Comput. Chem.* **2002**, *23*, 1391.
(31) Yamaguchi, Y. *J. Chem. Phys.* **2004**, *120*, 7963.
(32) Narioka, S.; Ishii, H.; Ouchi, Y.; Yokoyama, T.; Ohta, T.; Seki, K. *J. Phys. Chem.* **1995**, *99*, 1332.
(33) Tanida, H.; Nagatina, H.; Watanabe, I. *J. Chem. Phys.* **2003**, *118*, 10369.
(34) Khalil, M.; Marcus, M. A.; Smeigh, A. L.; McCusker, J. K.; Chong, H. H. W.; Schoenlein, R. W. *J. Phys. Chem. A* **2006**, *110*, 38 and references therein.
(35) Campbell, L.; Mukamel, S. *J. Chem. Phys.* **2004**, *121*, 12323 and references therein.
(36) Pandey, R. K.; Mukamel, S. *J. Chem. Phys.* **2006**, *124*, 094106.
(37) Boubekeur, K. *Acta Crystallogr.* **1995**, *C51*, 2244.